N94- 35611

Reduction Procedures for Accurate Analysis of MSX Surveillance Experiment Data

E. Mike Gaposchkin+, Mark T. Lane and Rick I. Abbot*

ABSTRACT

Technical challenges of the MSX science instruments require careful characterization and calibration of these sensors for analysis of surveillance experiment data. Procedures for reduction of Resident Space Object (RSO) detections will be presented which include refinement and calibration of the metric and radiometric (and photometric) data and calculation of a precise MSX ephemeris. Examples will be given which support the reduction, and these are taken from ground-test data similar in characteristics to the MSX sensors and from the IRAS satellite RSO detections. Examples to demonstrate the calculation of a precise ephemeris will be provided from satellites in similar orbits which are equipped with S-band transponders.

1.0 INTRODUCTION

The Midcourse Space Experiment (MSX) is scheduled for launch in 1994 and is a space flight program designed, in part, to demonstrate surveillance of the space and Resident Space Object (RSO) background from space (Mill et. al.). The technical challenges include cryogenic technology for cooling the Infrared sensor (SPIRIT III), low noise high performance focal planes, high off-axis stray-light rejection optics, on-orbit signal processing and data compression, and contamination control. The orbit is specified to be 898 km altitude circular at nearly a Sun-synchronous inclination of 99.16 degrees. The lifetime of SPIRIT III is expected to be 21 months, and the visible (SBV) and UV (UVISI) sensors have a planned operation period of 60 months. Primary science data will be stored on board using tape recorders and downlinked via 25 Mbit/s communications, and compressed science data will be downlinked via 1 Mbit/s communications. There will be two S-band transponders on board, which allow the S-Band Ground-Link Stations (SGLS) network to provide tracking data for precise ephemeris determination.

The SBV is the principal space surveillance sensor and uses a 15 cm aperture off-axis, re-imaging, all-reflective telescope, a thermo-electrically cooled, bare CCD focal plane, a signal processor and supporting electronics. The SBV focal plane contains four three side abuttable frame transfer CCDs with 420x420, 27μm pixels each. The design characteristics are given in Table 1.

Table 1: *SBV Characteristics*

Spectral Range	0.3000-0.9000 μm
Spatial resolution	12.1 arcsec (60 μrad)
Field of View	1.4° by 6.6°
Aperture, f/no.	15 cm, f/3
FPS size (four CCDs)	420 by 1680 pixels
Frame times	0.4,0.5,0.625,1.0,1.6,3.125 sec.
Quantum efficiency	28%

The SPatial Infrared Imaging Telescope (SPIRIT) 3 sensor is the primary instrument on MSX, covering the spectrum from the midwave infrared (MWIR) to the very-longwave infrared (VLWIR). SPIRIT III consists of an off axis re-imaging telescope with a 35-cm diameter unobscured aperture, a six-channel Fourier transform spectrometer, a five-band scanning radiometer, and a cryogenic dewar/heat exchanger.

+ Senior Staff Member, MIT Lincoln Laboratory, Lexington, MA 02173 (617)-981-3403

* Staff Members, MIT Lincoln Laboratory, Lexington, MA 02173 (617)-981-0973

This work was sponsored with the support of the Department of the Air Force under Contract F19628-90-C-0002. Review of this material does not imply Department of Defense endorsement of actual accuracy or opinion.

The sensitivity of the spectrometer limits its use for observing RSOs. The radiometer has five Si:As focal plan arrays of 8x192 pixels each, operating between 11 and 12 degrees Kelvin. It collects data in six color bands with a spatial resolution of 90 μradians. The scan mirror can remain fixed or can operate at a constant 0.46 degree/sec scan rate with programmable scan fields of 1x0.75, 1x1.15 and 1x3.0 degrees. The radiometer focal plane assembly uses a combination of dichroic and bandpass filters to allow simultaneous measurements in bands A, D and E, and in band B and C. The band B focal plane is divided horizontally into two equal sections, each with a slightly different bandpass. Table 2 lists the half-power bandpass, number of active columns, and projected sensitivity for each array. Similar to the SBV, there will be an Onboard Signal and Data Processor (OSDP) for clutter rejection and data compression.

Table 2: *SPIRIT III Radiometer Passbands*

Radiometer Bands	Band A	Band B1 Band B2	Band C	Band D	Band E
Passband (μm)	6.0-10.9	4.22-4.36 4.24-4.45	11.1-13.2	13.5-16.0	18.1-26.0
Active Columns	8	2	4	4	4
Sensitivity (NEFD) (10^{-18} W/cm^2)	1.1	10	0.8	0.7	1.7

The Ultraviolet/Visible Imaging and Spectrographic Imaging (UVISI) sensor system consists of five spectrographic imagers (SPIMS) and four imagers. Together the SPIMS cover a spectral range from far ultraviolet (110nm) to near infrared (900nm). The imagers include wide field-of-view (WFOV) and narrow-field-of-view (NFOV) sensors in the visible and ultraviolet. Surveillance investigations will concentrate on the NFOV imagers. The commandable filter wheel in each imager houses three bandpass filters and a neutral density filter, in addition to an "open" and "closed" position. The UVISI imager characteristics are given in Table 3.

Table 3: *UVISI Imager Characteristics*

Instrument	UV NFOV	Vis NFOV
FOV (deg)	1.28x1.59	1.28x1.59
Resolution (μ rad)	90	90
Passbands (nm)		
open	180-300	300-900
closed	--	--
ND filter	($x10^{-3}$)	($x10^{-4}$)
WB1 filter	200-230	305-315
WB2 filter	230-260	350-440
WB3 filter	260-300(polarization)	470-640

This report will focus on the reduction required for accurate analysis of the MSX space surveillance data. Three primary areas are identified: metric calibration, photometric and radiometric calibration, and calculation of the MSX precision ephemeris.

The SBV and SPIRIT III should provide metric measurements in the FK5 reference frame accurate to 15-20 micro-radians (3-4 arcseconds), and calibration will involve reference RSOs with well-known orbits (such as Lageos and EGP) and calibration of the sensor boresite, MSX fiducial reference frame, and sensor alignments. The UVISI sensors are not expected to provide high quality metric data.

The MSX sensors are designed to provide high quality radiometric data. The band-to-band ratios for calibrated SPIRIT III irradiance measurements are expected to be accurate to 5%. Radiometric calibration will involve RSO and stellar reference sources and multi-spectral comparisons from the different sensors.

The reduction of SGLS tracking data should provide an MSX orbit which is accurate to 15 meters. Obtaining this accuracy is difficult, however, and involves calibration of the SGLS tracking data, modeling of the MSX attitude and cryogen flow rate effects, and modeling other non-gravitational effects.

2.0 METRIC CALIBRATION

The SBV and SPIRIT III sensors should be able to provide good quality metric data. It is expected that the SBV metric data will be accurate to 4 arcseconds or better and that the SPIRIT III will be only slightly worse. This section will first describe the reduction that is required to produce the most accurate metric observations, and then techniques of calibrating the data will be presented involving the use of precise orbits of calibration RSOs. Test data similar to the SBV will be shown as examples of the reduction procedures and the means by which these data are calibrated.

2.1 Reduction of SBV Metric Data

The SBV involves highly distorted optics (which are not defraction limited) due to a design which attempts to maximize the rejection of stray light from the focal plane. The size of each pixel is approximately 13 arcseconds (60 micro-radians), and it is reasonable to try to sub-divide a pixel by a factor of 3-4 (or 4 arcseconds) using light which spills into neighboring pixels. SBV is a self-calibrating instrument, since it will be able to detect stars down to 15^{th} visual magnitude. Therefore, a precise inertial location of the boresite and attitude map can be determined for the SBV at any instance by matching star detections to a star catalog and fitting attitude model parameters to the star map. Then, once an attitude model is updated for the SBV, the model can be inverted to focal plane locations for an RSO detection to produce right ascension and declination measurements. A metric error budget for the SBV involves accuracy of the reference star positions and number of stars observed, centroid error from the observed stars in SBV focal plane coordinates, (streak) endpoint error from the observed RSO detections in SBV focal plane coordinates, and model error from the SBV distortion map.

Any catalog of reference stars can be used for SBV metric reduction, and we have chosen several. Each reference star is to be anchored to the FK5 inertial reference frame, and therefore stars which do not come in that frame must be carefully transformed. This is adequately detailed in (Smith et. al.). The catalogs which are currently implemented in the reduction software for the SBV are the SAO catalog, the Astrographic all-sky star catalog, the Guide Star catalog, and the Landolt Special Area Fields catalog (see Landolt). The Landolt catalog positions are not intended for metric use, but the color information is useful for photometric calibration of the SBV. Stars in the reference catalogs typically have position accuracy of 0.5 - 2 arcseconds, and the use of dense catalogs often allows more than 100 observed stars from the SBV to be matched. Both annual and diurnal aberration are applied to transform mean to apparent place for each reference star, because diurnal aberration can produce an effect on the order of 5 arcseconds due to the velocity of the MSX about the Earth. The parametric model for the SBV attitude and distortion involves 37 coefficients.

The SBV will have a signal processor on board the MSX, which will detect linear streaks moving from frame-to-frame across the focal plane and stationary light sources. If the SBV is commanded to observe in a Sidereal mode, then the stars in the background will be stationary and streaks may represent RSO targets. If the SBV is commanded to track a particular RSO, so that the RSO is stationary in the SBV focal plane, then stars will be seen as streaking across the focal plane. Because the SBV optics are not defraction limited, a stationary point source will spill into neighboring pixels and a streak will actually appear as a swath of pixels between 3 and 5 pixels wide. This works to our advantage, however, since centroiding will allow the reduction software to sub-divide a pixel by a factor of three or four. Based on ground calibration of the SBV sensor, it is estimated that centroid error is less than 0.2 pixels (or 2.6 arcseconds).

The direct map between inertial coordinates and pixel coordinates on a particular CCD in the SBV focal plane is accomplished by a series of coordinate frame rotations about angles which characterize the

SBV attitude. If **v** denotes an inertial unit vector and **w** a unit vector of direction cosines on the focal plane, the direct map is described mathematically as

$$\mathbf{w} = R_1(-\mu)R_2(\xi)R_3(\Psi+90)R_2(90-\delta_0)R_3(\alpha_0)\mathbf{v},$$

where R_k denotes the rotation about the axis k=1,2,3 by the indicated angle, α_0 denotes the SBV boresite right ascension, δ_0 the boresite declination, Ψ the SBV roll angle, and μ and ξ denote off-axis angles which are designed to move the boresite vector from the center of the SBV focal plane to the center of a particular CCD. Once **w** is calculated, direction cosines are input to the distortion map so as to convert (linear) direction cosines to CCD pixel coordinates.

The distortion map is expressed by a low-order polynomial in two direction cosine variables, U_z and U_y, involving 32 coefficients. The map can be described mathematically by

$$X_c = \sum_{m=0}^{15} a_m U_z^{p(m)} U_y^{q(m)}$$

and

$$Y_c = \sum_{m=0}^{15} b_m U_z^{p(m)} U_y^{q(m)},$$

where mathematical expressions for p(m) and q(m) are

$$p(m) = [\, m/4 \,]$$

and

$$q(m) = m - 4\,p(m)$$

with [k] being the integer portion of the number k. Initial calibration of the distortion map coefficients has been performed using the SBV optics on the ground, and it is found that this map is accurate to better than 0.15 pixels (or 2 arcseconds). The map described above can be inverted to transform pixel coordinates to inertial space, but the distortion map must be inverted using iterative techniques due to its non-linear nature.

2.2 Reduction of SPIRIT III Metric Data

In general, the SPIRIT III sensor will not be able to see enough stars in order to self-calibrate the pointing and attitude. Therefore, metric calibration will rely on alignment matrices between the SPIRIT III focal plane and an MSX fiducial frame. Alternatively alignment with the SBV focal plane can be used to determine the attitude of the SPIRIT III. The MSX is a rigid-body spacecraft, and there are no gimbaled mirrors. Therefore, pointing a sensor implies that the entire spacecraft must be pointed. The SPIRIT III and SBV sensors are co-aligned, and there exists a star camera on board the MSX which will be used to anchor the MSX fiducial frame. Whenever recognized stars are observed by the SPIRIT III, UVISI, and SBV sensors, then these data will be input to an algorithm to keep track of the alignment between sensors. This information will be steadily maintained throughout the lifetime of the instruments, and knowledge of the pointing for one sensor can be used in conjunction with the alignment information to determine the pointing for the other.

Distortion in the SPIRIT III optics will be modeled in a similar fashion to the SBV, and it is expected for the coefficients to change little from ground-calibration values since the temperature of the sensor will be kept nearly constant. Star data will be used periodically to check and update the SPIRIT III distortion model.

It remains to indicate how precise focal plane measurements of the RSO data are reduced from the SPIRIT III data. This task is performed by an On-Board Signal and Data Processor (or OSDP), which is to be

flown on board the MSX and can also be run on the ground with SPIRIT III raw data. The OSDP is a software and hardware system developed by the Hughes Aerospace Corporation, and involves two separate procedures. The first is known as the Time Dependent Processor, (TDP) which lines up the column data correctly from the SPIRIT III mirror scans (if necessary) and allows hot pixels to be grouped together. The second is known as the Object Dependent Processor (ODP), which detects a group of hot pixels and identifies star and streak data. These object sighting messages are prepared and attitude models are inverted for conversion into an inertial coordinate frame similar to the SBV detections.

2.3 RSO Calibration Orbits

Precision orbits of calibration RSOs are to be used to check the accuracy of the SBV and SPIRIT III metric data and to determine biases for the data. This section will identify RSOs that can be used for this procedure and will describe the independent data sets that are used to calculate the calibration orbits.

Good calibration RSOs are those which have stable orbits which are not difficult to model and which are routinely tracked by a variety of sites so that a dense sampling of tracking data is available. The Lageos calibration spheres are excellent candidates, because they are equipped with laser cube corner reflectors and serve as calibration RSOs for both radar and optical sites around the Globe. The Lageos orbits are stable and are routinely known to within 10 cm. They can also be routinely tracked by MSX sensors since viewing angles can be easily found which do not require tracking too close to the Sun or the Earth's limb. Other RSOs which make good calibration orbits are EGP, Etalon, ERS-1, and GPS. The GPS satellites make good calibration orbits because accurate samples of state vectors accurate to better than 5 m are available at all times.

The objective for calibrating the SBV and SPIRIT III data is to obtain an independent reference orbit for an observed calibration RSO which is accurate to better than 1 arcsecond in sensor right ascension and declination angles. The reference orbit is calculated using a special perturbation orbit determination program which can fit many types of data to the equations of motion using a detailed force model. Then this orbit is compared to the observed data and statistics are calculated from the pass. Biases are included in a historical database and incorporated into the calibration models for the metric data reduction.

The precision orbit determination software which is used for this procedure is known as DYNAMO, and it has a history dating back to the 1960s for use in calibrating sensor data and providing precision reference orbits. The capabilities and qualities of DYNAMO are highlighted in Figure 1.

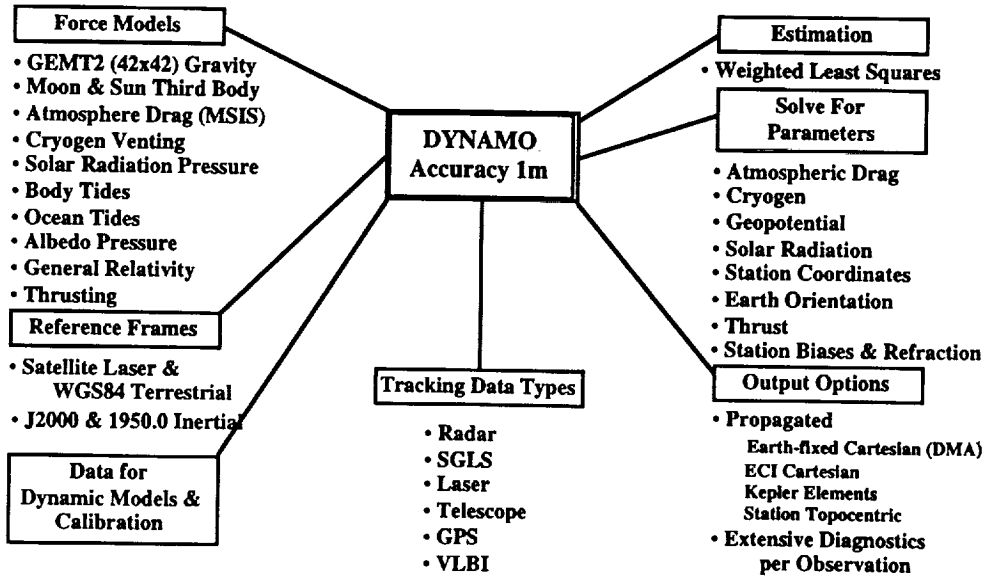

Figure 1: *DYNAMO, A Precision Orbit Determination Software Package*

2.4 Example of Metric Reduction and Calibration

In this section, an example of the metric reduction and calibration process will be presented. The raw data for this example are selected from a ground-test setup designed to be similar to the SBV. A 6 inch telescope system was attached to the 31 inch optical mount at the Experimental Test Site (ETS), located near Socorro, New Mexico. A 420 x 420 CCD focal plane was used to record the data employing parameters for the integration time and number of frames which are similar to the SBV. In November of 1991, a 32 minute pass of the Lageos I satellite was collected with this system using 29 sets of data with 8-16 frames for each set. The reduction and calibration steps for this set of data will be highlighted in this section, with the final objective being to characterize the accuracy of Lageos I metric observations.

First, the raw data must be passed through the SBV Signal Processor to detect the stationary point sources and streaks. In addition to the streak metric information, a type of signature data must be collected which labels frame and intensity data for each pixel near the best-fit line to the streak. The signature information is used in post-processing to refine the end points and deduce a visual magnitude measurement for each streak detection.

The next step is to match as many of the observed stars as possible to an on-line star catalog and to update attitude parameters for the sensor (boresite vector and focal plane scale). The results are shown in Figure 2, displaying a Bull's-eye plot of the residuals (in the focal plane) of the stellar position data after the fit. This chart shows that the root mean square (rms) of the residuals is close to 1 arcsecond in each direction. Outliers can be traced to saturation, double-star systems, or stars which are on the edge of the field of view.

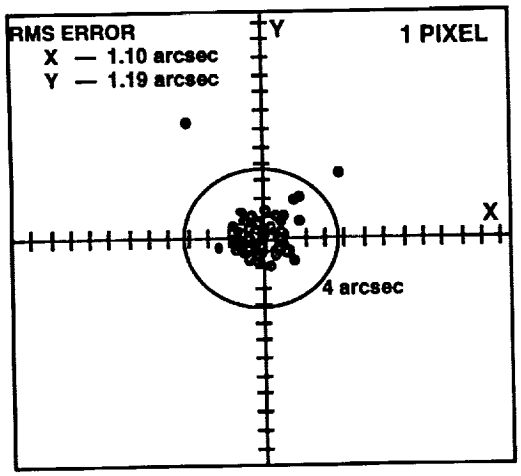

Figure 2: *Bulls-Eye Plot of Residuals (arcseconds) of Matched Star Positions Based on a Least Squares Fit of the Focal Plane Attitude Parameters*

Once an accurate attitude map is available, the end points of the observed streak must be refined using the signature data and the attitude map must be inverted to transform the streak end point measurements in focal plane coordinates to inertial right ascension and declination measurements. In order to characterize these measurements, a precision ephemeris for Lageos I must be determined. This is accomplished using DYNAMO and independent measurements of Lageos I from a time period spanning plus or minus three days about the epoch of the pass. The independent measurements are taken from laser radar and skin tracking from radars and optical sites in the Space Surveillance Network. This suite of observations allows an ephemeris for Lageos I to be determined to better than 10 cm, and this implies that the predicted sensor accuracy from a ground-based site is better than a fraction of an arcsecond. A comparison of the Lageos I observations to the precision ephemeris is shown in Figure 3. There is a strong bias in declination of

2.2 arcseconds, and this could be due to a time discrepancy since the inclination of Lageos I (109 degrees) causes along track orbit error to be manifested as a declination error. The standard deviations in right ascension and declination are larger than the desired 4 arcseconds, and the principal sources of error are not easily identified. Possible error sources include a (slight) shift of the mount from frame to frame and noise in the data.

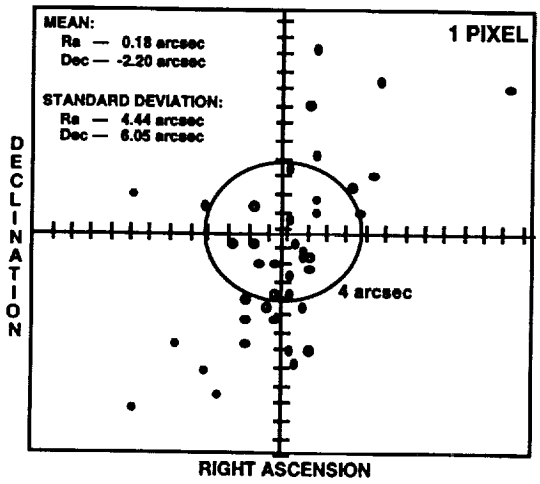

Figure 3: *Bulls-Eye Plot of Residuals (arcseconds) of Lageos I Metric Observations as Compared to a DYNAMO Reference Orbit for a 32 Minute Pass.*

3.0 RADIOMETRIC CALIBRATION

3.1 Introduction

The SBV, SPIRIT III, and UVISI sensors should be able to produce high quality photometric and radiometric data. Surveillance data will be used with high fidelity models of the reflected and self-emitted radiation from satellites, to develop methods for identifying RSOs, monitoring their status, and determining some of their physical properties. These high fidelity models account for such variables as: solar phase angle, sensor to RSO aspect angle, material properties, and temperature. The discussion here is limited to the methods of data reduction and calibration to be used with each of the MSX sensors, and an assessment of the expected accuracy.

Each of the MSX sensors is unique, and the data reduction and calibration will be different for each one. The MSX program intends to provide data that is certified to be calibrated to within specified limits. To this end, the Data Certification And Technology Transfer (DCATT) Principal Investigator Team is devoted to establishing calibration procedures and standard data reduction software. Even though fundamental differences between the MSX instruments require different calibration and data reduction methods, they do share some common elements. For example, there are three steps in the calibration process. Each instrument will have extensive preflight (or bench) calibration. It is hoped that this preflight calibration will be valid for the on-orbit data. Second, there will be a series of on-orbit observations taken for purposes of calibration. These include internal sources, used in each data set, to obtain corrections for each data set. Finally, some data sets will contain observations of objects with known luminosity, which will provide additional calibration information. These three sources of information will provide the calibration information necessary for photometric and radiometric analysis of MSX data.

3.2 SBV Radiometric Reduction and Calibration

The conversion of raw digital numbers to engineering units for the SBV is done for each pixel. The dark current (a function of temperature) is measured with the SBV cover closed, and is subtracted from the measurement. The responsivity conversion of digital numbers to Watts/cm^2 in band is done using ground-based calibration data.

The on-orbit calibration phase will be done using calibrated reference stars, primarily the Landolt fields (Landolt). The Landolt star fields have been established as astronomical photometric calibration standards. Since the SBV has a nonstandard and very broad spectral response, the relation between the SBV magnitude and the magnitude of a star must be known. From analysis of the SBV spectral response, the relation between the visual magnitude of a star, M_v, with color, B-V, and the SBV magnitude, M_{SBV} is given by an empirical relation (Beavers)

$$M_{SBV} = M_v + R_1(B\text{-}V) + R_2(B\text{-}V)^2 + R_3(B\text{-}V)^3 .$$

We expect this relation be have an accuracy better than 0.02 magnitude.

During the collection of RSO science data, many observed stars will have a visual magnitude and a color, though not of the accuracy and reliability as the Landolt calibration fields. The process of reducing the SBV data will start with a computed value, M_{SBV}^{cat} (as described above), for each detected star found in the star catalogue, and this is compared with the observed magnitude, M_{SBV}^{obs}, derived from the calibration. The mean difference between these two quantities becomes the zero-point correction for the frame set,

$$\Delta M_{SBV} = \Sigma (M_{SBV}^{obs} - M_{SBV}^{cat}) / n$$

and is subtracted from the observed RSO magnitude. In this way the SBV makes self- calibrating photometric measurements.

In processing SBV photometric data, a simple model is used for prediction of M_{SBV}^{RSO}. It is based on assuming that the satellite reflects the solar spectrum. We have adopted (Beavers)

$$M_{SBV}^{RSO} = -26.8 - \log_{10} (\rho A F(\phi) / r^2)$$

where ρ is the reflectivity, A is the effective area, $F(\phi)$ is the phase function, and r is the range to the target.

As an example of this process, a comparison of a pass of SBV like data taken on the Lageos satellite at the Lincoln Laboratory Experimental Test Site (ETS) is given in Table 4. This 32 minute pass is from the same example data discussed in the Section 2.4 on metric calibration, and photometric measurements were computed using the signature data collected by the SBV signal processor. These data were used to determine M_{SBV}^{RSO} using a zero-point correction calibrated by the stars, as described above. The area and reflective properties of the Lageos I sphere are used in the model. Shown in Table 4 are the solar phase angle and the residuals in SBV magnitude for each of the Lageos observations from the data set described in Section 2.4. The visible model used ρ=0.15 for the reflectivity, A=0.5 m^2 for the effective area of the sphere, and $F(\phi)=2((\pi - \phi)\cos(\phi) + \sin(\phi))/(3\pi^2)$ for a diffuse sphere. The results illustrate modeling the photometric properties of Lageos sample to better than 0.4 magnitudes.

3.3 SPIRIT III Radiometric Reduction and Calibration

The on-orbit calibration phase for SPIRIT III will be done in two different ways. First, a ground based observing program has been conducted to determine a small number of stellar infrared reference calibration sources. These sources will be routinely observed and used to monitor the stability of the infrared sensor. As described below, calibration and analysis of infrared data involves knowledge of the source

temperature. For a star, the irradiance as a function of temperature depends in a fundamental way on the composition of the stellar atmosphere, a subject still under development. This proved to be an important issue in the calibration of IRAS (Beichman et.al.). Therefore stars will provide a stable reference to monitor a change in the sensor, but another calibration method will be used. There are five emissive reference spheres that will be deployed from the MSX during the SPIRIT III lifetime. These two centimeter spheres, coated with Martin Black, are designed to have a well defined temperature, and to provide orbital geometry that will sample the full dynamic range of the SPIRIT III. The goal is to provide knowledge of the emissive reference sphere temperature with sufficient accuracy to determine the absolute irradiance to 15% and the band-to-band ratio to 5%.

Table 4: *Comparison of an Observed Pass of Visible Data for Lageos with a Photometric Model*

							SENSOR MAGNITUDES		
OBJECT	YR	DAY	HR	MN	PHASE	RANGE	OBS	PRED	RES
8820	91	312	2	6	+ 26.1	7581.1	12.10	12.21	-0.11
8820	91	312	2	6	+ 25.6	7548.4	11.98	12.20	-0.22
8820	91	312	2	6	+ 25.3	7534.7	11.93	12.19	-0.26
8820	91	312	2	7	+ 24.4	7480.7	12.10	12.17	-0.07
8820	91	312	2	8	- 22.7	7382.1	11.72	12.13	-0.41
8820	91	312	2	8	- 22.7	7382.1	11.58	12.13	-0.55
8820	91	312	2	9	- 21.6	7312.9	12.02	12.10	-0.08
8820	91	312	2	9	- 20.9	7270.0	12.13	12.08	0.05
8820	91	312	2	15	- 17.9	6880.7	11.71	11.95	-0.24
8820	91	312	2	16	- 18.7	6851.9	11.92	11.94	-0.02
8820	91	312	2	18	- 20.7	6814.4	11.90	11.94	-0.04
8820	91	312	2	18	- 21.7	6804.7	11.88	11.95	-0.07
8820	91	312	2	19	- 22.9	6798.8	11.76	11.95	-0.19
8820	91	312	2	20	- 25.0	6798.1	11.55	11.97	-0.42
8820	91	312	2	21	- 27.0	6806.4	11.54	11.99	-0.45
8820	91	312	2	22	- 29.2	6823.4	12.06	12.01	0.05
8820	91	312	2	23	- 31.6	6850.9	12.13	12.04	0.09
8820	91	312	2	24	- 34.2	6891.0	12.53	12.08	0.45
8820	91	312	2	25	- 36.3	6930.2	12.80	12.11	0.69
8820	91	312	2	26	- 38.6	6981.5	12.67	12.15	0.52
8820	91	312	2	27	- 41.2	7045.6	12.81	12.20	0.61
8820	91	312	2	28	- 43.6	7114.7	12.37	12.26	0.11
8820	91	312	2	37	- 64.2	8068.4	13.55	12.86	0.69
8820	91	312	2	38	- 65.2	8131.8	13.24	12.90	0.34

For surveillance data analysis, a simplified calculation is needed for the automated processing and a quick check of the observed RSO radiometry. The following describes such a process. Tables have been developed for processing the six SPIRIT III wavebands and the four IRAS wavebands. These can be augmented for other wavebands as necessary. The analysis involves conversion of the input observation for each band in Watts/m^2 in band to any other band, and conversion to standard units such as Jansky's (W/m^2/Hz) and Naj's (W/m^2/micron). The basic relations are as follows: If the telescope response is $R(\lambda)$, the filter + blocker + detector response for band B is $\tau_B(\lambda)$, the Planck function radiation is $\Im_\lambda(T)$, and T is the absolute temperature, then we define *the object in-band radiance* as

$$F^B(T) = \int_0^\infty R(\lambda)\tau_B(\lambda)\Im_\lambda(T)\,d\lambda \qquad \left(\frac{W}{m^2}\right)$$

where the Planck flux density is

$$\Im_\lambda(T) = \frac{3.74185 \times 10^8}{\lambda^5\left(e^{\frac{14388.3}{\lambda T}} - 1\right)} \qquad \left(\frac{W}{m^2\mu}\right)$$

and λ is in microns (Allen). For convenience we call this flux density unit a Naj. A generally used alternate flux density unit is the Jansky defined as 10^{-26} W/m^2/Hz. Using the relation that $f\lambda=c=2.99792458\times10^{14}$ microns/sec, we can convert Naj's to Jansky's with Naj's=Jansky's*$2.99792458\times10^{-12}/\lambda^2$. We can now compute the observed flux (in-band) irradiance as

$$F_0^B(T) = \frac{\varepsilon A}{\pi r^2}\int_0^\infty R(\lambda)\tau_B(\lambda)\Im_\lambda(T)\,d\lambda \qquad \left(\frac{W}{m^2}\right),$$

where A is the area of the object, ε the emissivity, and r the range to the object.

The temperature of an object can be found as follows. The temperature dependence of the observed flux, $F_o^B(T)$, depends on the band. It also depends on ε,A, and r. Assuming ε is independent of λ, the ratio

$$\Re(T) = \frac{F_0^x(T)}{F_0^y(T)} = \frac{F^x(T)}{F^y(T)}$$

for bands x and y, is a monotonic function of T. Figure 4 displays this ratio for a number of bands for the SPIRIT III sensor. Therefore, given this function an observed in-band flux ratio immediately determines the temperature, independent of object size, range, and emissivity. With the measurement of n in band fluxes, n(n-1)/2 determinations of temperature are possible.

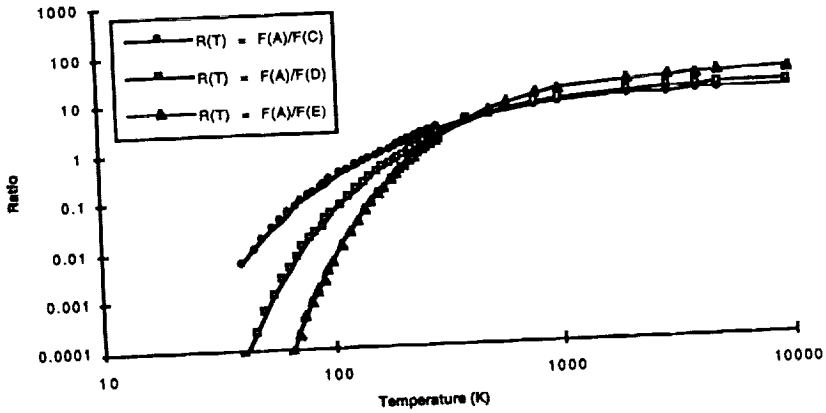

Figure 4: *Ratio of Flux Densities for SPIRIT III Wave Bands*

Given a temperature, the observed in-band flux can be expressed in Naj's at a reference wavelength, λ_o, as

$$N_0^{\lambda_0} = F_0^B\left(\frac{\Im_{\lambda_0}(T)}{F^B(T)}\right) \qquad \left(\frac{W}{m^2\mu}\right)$$

It is customary (though not necessary) to select λ_o in the band. This can be converted to Jansky's, as described above, with

$$J_0^{\lambda_0} = N_0^{\lambda_0}\left(\frac{\lambda_0^2}{2.99792458 \times 10^{-12}}\right)$$

As an example of this process, we show some data from the IRAS satellite. The InfraRed Astronomy Satellite (IRAS) was operational for about 10 months in 1983. The IRAS sensitivity is very similar to that expected from SPIRIT III, although the IRAS observing geometry resulted in measurements at a phase angle near 90 degrees. However, a number of observations on medium to high altitude satellites were made over the lifetime of IRAS, and they are illustrative. In Table 5, we give the results of analysis of an observation sequence for the Lincoln Calibration Sphere (LCS) 1 (SSC #1361). This is a 1 meter square area sphere in a circular orbit at a range of 1900 km. Three measurements were taken in each of the 12, 25, and 60 micron bands, and if a value of ε= 0.032 is used, then we see the comparison of the measurements to the model is good to better than 0.5 Jansky's. The largest residual is for the 60 micron measurement, and the temperature inferences from the ratios with this measurement appear to be high. It is reasonable for this

methodology to be able to provide temperature data from SPIRIT III measurements to ±5°K in temperature and ±2% in emissivity and absorbtivity.

3.4 UVISI Radiometric Reduction and Calibration

The on-orbit calibration phase for UVISI will be done using calibrated reference stars. There are two issues involved here. The first is the algorithm for detecting and extracting the aperture irradiance. In contrast to the SBV, a star will generally fall in only one pixel. The detection will be based on finding the pixels with exceedences greater than some threshold and correlation with detections from the SBV signal processor. Secondly, since the UVISI has a non-standard spectral response, the relation between the UVISI magnitude and the magnitude of a star must be known. From analysis of the UVISI spectral response, the relation between the visual magnitude of a star, M_v, with color, B-V, and the UVISI magnitude, M_{UVISI} is given by an empirical relation similar to that for M_{SBV} (Beavers).

Table 5: *Comparison of an Observed Pass of IRAS Infrared Data for LCS-1 with a Radiometric Model*

							CORRECTED JANSKYS			FLUX DATA (W/SQ METER)		
OBJECT	YR	DAY	HR	MN	BND	RANGE	OBS	PRED	RES	OBS	PRED	RES
1361	83	72	11	56	I12	2001.1	16.55	16.42	0.132	0.11E-11	0.11E-11	0.89E-14
1361	83	72	11	56	I25	2001.1	8.97	8.75	0.212	0.29E-12	0.28E-12	0.68E-14
1361	83	72	11	56	I60	2001.1	1.82	2.27	-0.449	0.11E-13	0.14E-13	-0.27E-14
3 TEMPERATURE MEASUREMENTS:							479.51	561.76	958.71			

During the collection of RSO science data, each UVISI frame will detect many stars will have a visual magnitude and a color, though not of the accuracy and reliability as the calibration fields. The process of reducing the UVISI data will be similar to SBV: Compute M_{UVISI}^{cat} for each detected star found in the star catalogue and compare with the observed magnitude, M_{UVISI}^{obs}, derived from the calibration. The mean difference between these two quantities becomes zero-point correction for the frame,

$$\Delta M_{UVISI} = \Sigma (M_{UVISI}^{obs} - M_{UVISI}^{cat}) / n$$

and is subtracted from the observed RSO magnitude. In this way the UVISI makes self- calibrating photometric measurements, similar to the SBV.

In processing UVISI photometric data, a simple model is used for prediction of M_{UVISI}^{RSO}. It is based on assuming that the satellite reflects the solar spectrum. We have adopted (Beavers)

$$M_{UVISI}^{RSO} = -26.8 - \log_{10} (\rho A F(\phi) / r^2) + \Delta M ,$$

where ρ is the reflectivity, A is the effective area, $F(\phi)$ is the phase function, and r is the range to the target. The function ΔM will color correct the model for each UVISI waveband.

4.0 THE MSX EPHEMERIS

4.1 Description of the Problem and Method of Attack

The metric accuracy of the MSX sensors critically depends on the ephemeris or position accuracy of the MSX satellite platform. This section will be describe the required ephemeris accuracy for the MSX and how it can be achieved.

The ephemeris accuracy requirements are dependent on the required metric data quality for the SPIRIT III and SBV. It is required that the ephemeris error for MSX be a small part of the overall error budget, and (more specifically) 3-10 times less than the error of the data. An example of one of the more stressful demands on the MSX ephemeris accuracy will be when the SBV or SPIRIT III is viewing an object at the Earth's tangent height, a range 2500 km, in a 90 minute parking orbit. A simple calculation indicates

that with 4-arcsecond sensor data quality and a requirement that the ephemeris error be at least 3 smaller implies that the ephemeris accuracy for MSX must be better than 15 meters.

There were three methods considered for providing the required ephemeris accuracy: 1) an on-board GPS receiver, 2) ground (or skin) tracking from the Space Surveillance Network (SSN) radars, or 3) ground tracking from the Air Force S-band Ground Link Stations (SGLS). A GPS receiver on board the MSX was the most attractive choice; but it was eliminated because of power, weight, and space requirements. Radar (skin) tracking of the required accuracy could come from the Millstone radar in Massachusetts and from the ALTAIR radar in the Marshall Islands (in the near equatorial Pacific). These provide accurate enough measurements, but they are heavily tasked already and the amount of tracking that would be required for MSX would demand too much of their resources. The SGLS network is used by the Air Force for satellite communications, and the S-band tracking data is obtained to support acquisition. The MSX satellite will have a coherent S-band transponder and will be controlled by the SGLS network. Tracking data from this network become an attractive source for calculating a precision ephemeris for the MSX. The SGLS network is a globally distributed network of stations, measuring range, range rate, azimuth, and elevation for satellites with a coherent transponder.

To determine if the SGLS tracking data could suitably meet the 15 meter accuracy requirement for MSX, a number of evaluations of the data have been made. The original studies were made in late 1989 and through 1990. These studies involved SGLS data from two satellites with similar orbital parameters to MSX. Table 6 compares these with one column devoted to the expected orbital parameters for MSX. The two test satellites were lower, however, and their attitudes were not well-determined, which implied that atmospheric drag was more difficult to model than is expected for MSX. The remaining dynamical complication that could not be considered during these tests arises from the fact that MSX will have cryogen gas venting during the useful lifetime of the SPIRIT III sensor. This phenomenon will constitute a significant perturbation of the MSX orbit and is absent in the test satellites.

Table 6: *Orbit Comparison of MSX and the Evaluation Test Objects: #19911 and #20497*

	MSX	19911	20497
ALTITUDE (km)	888.	490.	460.
ECCENTRICITY	0.001	0.00133	0.00161
INCLINATION (deg)	99.	47.7	43.1
DRAG	YES	HIGH	HIGH
MANEUVER	NO	OFTEN	NO
SATELLITE ASPECT	KNOWN	NOT KNOWN	NOT KNOWN

The objectives of the sample evaluations were to establish how accurately an orbit could be determined for the two satellites with SGLS data. The stated precision of SGLS data is 6 meters in range, 3 cm/s in range rate, and 20 millidegrees for the angle measurements. These values are potentially good enough to meet the orbit accuracy requirements. Related questions which were addressed by the test evaluations include: how much tracking is required?, how well are the data calibrated?, and what additional processing has to be done in order to use the data to its potential?

The late 1989 and 1990 studies took place during periods of major solar activity. For these low altitude satellites, it was found that three day orbit fits were most suitable for the SGLS data. Besides solving for the satellite state vector, drag scale factors at half day intervals were also estimated. The orbit accuracy was evaluated using high accuracy radar measurements and also by comparing overlapping orbits. The radar measurements were from the Millstone Hill L-Band radar (with a range accuracy of 1 meter) and from the ALTAIR UHF radar (with a range accuracy of 10 meters).

The SGLS data had a nominal range bias correction applied (none for the angles) and a troposphere refraction correction based on an empirically derived mapping function and monthly surface refractivity values. No ionosphere refraction correction had been applied, and so we applied corrections based on the best

available global model (Bilitza, Klobuchar). The range rate had to be converted to a range difference measurement to be properly used. Additional biases in the range data were determined thereby improving the calibration and accuracy of the data. The angles were also calibrated.

With an enhanced calibration and an average of 8 tracks per day, the evaluation showed that the two satellites have orbits computed to an accuracy of 15 meters. This is illustrated in Figures 6 and 7. Figure 6 provides a sample of the data quality from one of the SGLS tracking stations (Guam) using an orbit computed with the radar data, and Figure 7 shows range residuals for the radar data using an orbit computed with the SGLS data. The plots display the mean and +/- 1 σ error bars for each of the tracks. The means from Figure 7 are within 15 meters and are due to a combination of measurement error and orbit error. These evaluations indicate that the SGLS network can provide the necessary tracking data for the MSX orbit computation.

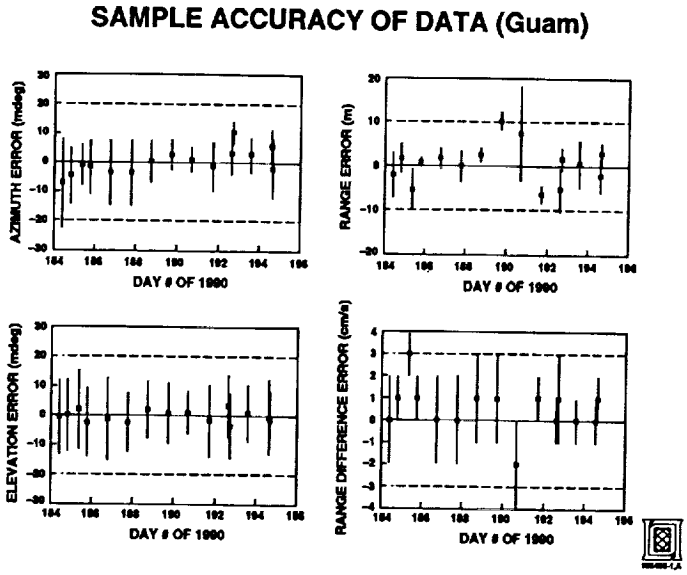

Figure 6: *Residuals of SGLS Tracks from an Orbit Determined with Radar Data*

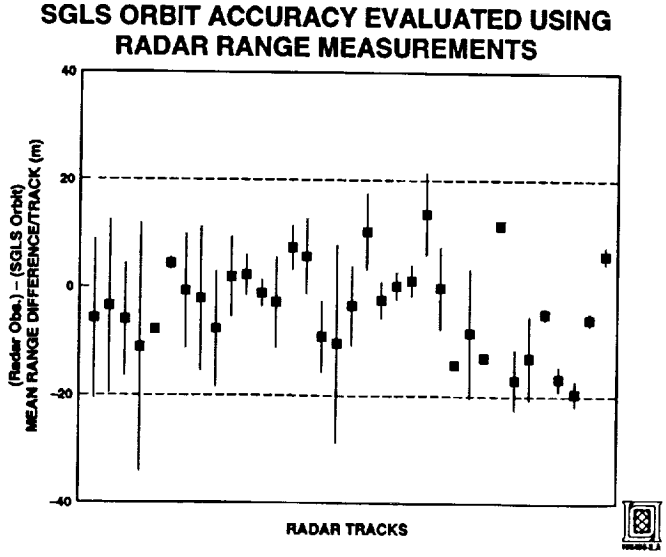

Figure 7: *Residuals of Radar Tracks from an Orbit Determined with SGLS Data*

4.2 Modeling the MSX Orbit

In order to produce a 15 meter orbit for the MSX on a routine basis, accurate modeling of the forces acting on the MSX orbit is required. The gravitational forces are well known and already incorporated in the DYNAMO software. The non-conservative forces which are more difficult to model include radiation pressure, atmospheric drag, and the force induced by the venting of the gas created by the sublimation of a solid hydrogen block within the cryo-stat. Two important data types that must be obtained and input to the MSX force model are the satellite attitude and the venting flow rate of hydrogen gas from the cryogen cooling system. The attitude data is necessary for the drag, solar radiation pressure, and cryogen venting models. The cryogen flow rate data will be measured and provided by Utah State University (the manufacturers of SPIRIT III), and details are still being worked out.

The cryogen gas venting model is the remaining dynamical complication for the MSX satellite. The cryo-system on the MSX contains a large mass of solid hydrogen, which is used to keep the instruments at the required temperature. As heat is added to or generated by the satellite, the hydrogen escaping through the venting system produces a low thrust on the satellite. Depending on the detailed geometry of the venting system, the effect of the resulting force can be large when integrated over the course of a day. Details on the exact nature of this force are yet unclear, but an exact or an empirical model (which will be parametrized and updated from the orbit fits) is critical to achieving a 15 meter orbit for the MSX on a routine basis.

5.0 SUMMARY

The MSX science instruments cover a wide range of the spectrum from the ultra-violet to the long-wave infrared and will be able to provide useful metric, photometric, and radiometric data for surveillance of the Resident Space Object background. Careful characterization and calibration of the sensor data is required for accurate analysis of space surveillance experiment data. Procedures for reduction and refinement of the metric and radiometric (or photometric) data have been presented and methods of calibration have been described. Examples from ground-test data similar in characteristics to the MSX sensors and from the IRAS RSO detections have been presented to support the reduction and procedures outlined in this report. In addition to the reduction of the MSX sensor data, it is crucial to calculate a precise MSX ephemeris. The ephemeris is calculated using SGLS tracking of data from one of two S-band transponders on board the MSX and sophisticated models of the MSX orbit. Examples to demonstrate the techniques for this calculation have been provided from satellites in similar orbits equipped with S-band transponders.

6.0 REFERENCES

- Allen, C.W., **Astrophysical Quantities**, The Athlone Press, London, 310pp, 1973.
- Beavers, W., Private Communication, 1989.
- Beichman, D., *Infrared Astronomical Satellite (IRAS) Catalogs and Atlasses. Vol I: Expanatory Supplement*, Jet Propulsion Laboratory, NASA RP-1190, 455pp., 1987.
- Bilitza, D., *International Reference Ionosphere: Recent Developments*, Radio Sci., **21**, 343, 1986.
- Klobuchar, J.A., Private Communication, 1989.
- Landolt, A., *UBVRI Photometric Standard Stars in the Magnitude Range 11.5 < V < 16.0 Around the Celestial Equator*, Astron. J., **104**, 340 - 371, July, 1992.
- Mill, J.D., O'Neil, R.R., Price, S., Romick, G.J., Uy, O.M., Gaposchkin, E.M., Light, G.C., Moore Jr., W.W., and Murdock, T.L., *The Midcourse Space Experiment: Introduction to the Spacecraft, Instruments, and Scientific Objectives*, J. Rockets and SpaceCraft, In Press, 1994.
- Smith, C.A., Kaplan, G.H., Hughes, J.A., Seidelmann, P.K., Yallop, B.D., and Hohenkerk, C.Y., *Mean and Apparent Place Computations in the New IAU System. I. The Transformation of Astrometric Catalog Systems to the Equinox J2000.0*, The Astron. J., **97**, 265-273, January, 1989.
- Wyatt, C.W., *Acceptance Test Data and Algorithms for Predicting SPIRIT III Radiometric Performance*, SDL/92-048, Space Dynamics Laboratory/Utah State University, Logan Utah, June, 1992.

FLIGHT MECHANICS/ESTIMATION THEORY SYMPOSIUM

MAY 17-19, 1994

SESSION 2